Physics Letters B 822 (2021) 136645

Contents lists available at ScienceDirect

Physics Letters B

www.elsevier.com/locate/physletb

Evidence of oblate-prolate shape coexistence in the strongly-deformed nucleus ^{119}Cs

K.K. Zheng [a,b], C.M. Petrache [a,*], Z.H. Zhang [c], P.W. Zhao [d], Y.K. Wang [d], A. Astier [a], B.F. Lv [a,b], P.T. Greenlees [e], T. Grahn [e], R. Julin [e], S. Juutinen [e], M. Luoma [e], J. Ojala [e], J. Pakarinen [e], J. Partanen [e], P. Rahkila [e], P. Ruotsalainen [e], M. Sandzelius [e], J. Sarén [e], H. Tann [e,f], J. Uusitalo [e], G. Zimba [e], B. Cederwall [g], Ö. Aktas [g], A. Ertoprak [g], W. Zhang [g], S. Guo [b,h], M.L. Liu [b,h], I. Kuti [i], B.M. Nyakó [i], D. Sohler [i], J. Timár [i], C. Andreoiu [j], M. Doncel [f], D.T. Joss [f], R.D. Page [f]

[a] Université Paris-Saclay, CNRS/IN2P3, IJCLab, 91405 Orsay, France
[b] Key Laboratory of High Precision Nuclear Spectroscopy and Center for Nuclear Matter Science, Institute of Modern Physics, Chinese Academy of Sciences, Lanzhou 730000, China
[c] Mathematics and Physics Department, North China Electric Power University, Beijing 102206, China
[d] State Key Laboratory of Nuclear Physics and Technology, School of Physics, Peking University, Beijing 100871, China
[e] University of Jyväskylä, Department of Physics, P.O. Box 35, FI-40014, University of Jyväskylä, Finland
[f] Oliver Lodge Laboratory, Department of Physics, University of Liverpool, Liverpool L69 7ZE, United Kingdom
[g] KTH Department of Physics, S-10691 Stockholm, Sweden
[h] School of Nuclear Science and Technology, University of Chinese Academy of Science, Beijing 100049, China
[i] Institute for Nuclear Research (Atomki-ELKH), 4001 Debrecen, Hungary
[j] Department of Chemistry, Simon Fraser University, Burnaby, BC V5A 1S6, Canada

ARTICLE INFO

Article history:
Received 27 April 2021
Received in revised form 2 August 2021
Accepted 12 September 2021
Available online 16 September 2021
Editor: B. Blank

Keywords:
Nuclear reaction: ^{58}Ni(^{64}Zn,3p)^{119}Cs
Measured $\gamma\gamma\gamma$-coincidences
Angular correlations
Linear polarization
Model calculation
Oblate-prolate coexistence

ABSTRACT

Prolate-oblate shape coexistence close to the ground state in the strongly-deformed proton-rich $A \approx 120$ nuclei is reported for the first time. One of the four reported bands in ^{119}Cs, built on a $11/2^-$ state at 670 keV, consists of nearly degenerate signature partners, and has properties which unequivocally indicate the strongly-coupled $\pi h_{11/2}[505]11/2^-$ configuration associated with oblate shape. Together with the decoupled $\pi h_{11/2}[541]3/2^-$ band built on the $11/2^-$ prolate state at 110 keV, for which a half-life of $T_{1/2} = 55(5)$ μs has been measured, the new bands bring evidence of shape coexistence at low spin in the proton-rich strongly deformed $A \approx 120$ nuclei, a phenomenon predicted since long time, but not yet observed. Calculations using the particle-number conserving cranked shell model and two dimensional tilted axis cranking covariant density functional theory support and well reproduce the observed oblate and prolate coexisting low-energy states in ^{119}Cs.

Nuclei with an oblate ground state are far more rare than those with prolate shapes. A competition between oblate and prolate shapes at low spin is present in limited regions of the nuclear chart, around proton-rich Pb [1,2], Hg [3,4], and $A \approx 70$ nuclei [5,6]. At high spin, various types of oblate bands are known: superdeformed and normal deformed rotational bands in several mass regions [7], regular dipole bands in $A \approx 130$ nuclei [8], bands evolving from prolate to oblate shape in neutron-rich Hf nuclei [9]. Recently, an extremely stable rotational band in ^{137}Nd, extending ≈ 5 MeV above yrast at the highest spins, has been interpreted as collective rotation of a nucleus with oblate shape [10]. Nonetheless, the number of experimentally observed oblate bands is very limited. In particular, no oblate bands have been observed in the strongly-deformed proton-rich $A \approx 120$ nuclei, even though predictions exist since long time, based on calculations employing various interactions [11–13]. Potential energy surfaces calculated e.g. with the Gogny D1S interaction [14], exhibit coexisting prolate and oblate minima for ^{118}Xe and ^{120}Ba, which are the cores of the nucleus of interest of the present letter, ^{119}Cs. The relative excitation and deformations of the minima depend on the employed single-particle interaction, but in general the oblate minimum has an excitation energy within 1 MeV relative to the ground state, is

* Corresponding author.
E-mail address: petrache@csnsm.in2p3.fr (C.M. Petrache).

https://doi.org/10.1016/j.physletb.2021.136645

more narrow and has a smaller deformation than the prolate minimum. The theoretical calculations for odd-even nuclei are more scarce [15,16]. Aggarwal predicted oblate ground states for ^{115}Cs and ^{117}La [16].

Oblate shapes can be induced by large energy gaps, like those at $Z = 56$ and $N = 60$ above $Z = 50$ major shell, and favored by the presence close to the Fermi surfaces of high-Ω Nilsson orbitals which have strong driving force towards oblate shape. The proton-rich $A \approx 120$ nuclei are among the best cases for oblate ground states, mainly due to the $\pi[505]11/2^-$ orbital, which has the steepest slope as a function of quadrupole deformation: when coupled with an oblate core, can give rise to strongly-coupled bands composed of degenerate signature partners which can develop over extended spins ranges, enabling thus the study of their properties. However, no experimental evidence of such low-lying oblate bands in proton-rich $A \approx 120$ nuclei has been reported so far. The present letter gives a positive answer to the question related to the existence of oblate shapes induced by the strongly oblate-driving orbitals like $\pi[505]11/2^-$.

This missing experimental evidence can be explained by the low barrier between the prolate and oblate minima, and by the strong pairing correlations at low excitation energy, which induce strong mixing and fragmentation of the wave functions, prohibiting thus the development of long rotation cascades.

However, in odd-even nuclei, the angular momentum of the odd nucleon can have very different orientations relative to the core, and can give rise to K isomers, which can facilitate the observation of oblate states [15,16]. One or two long-lived isomeric states were identified long time ago in Cs nuclei [17], and their magnetic moments and spectroscopic quadrupole moments were measured [18]. All these isomers were assigned to prolate shapes, with deformations increasing towards the drip line. However, the predicted oblate states can have lifetimes too short to allow their identification using isotope separation online methods.

The present letter reports for the first time the discovery of an oblate negative-parity band in the proton-rich strongly-deformed nucleus ^{119}Cs, the determination of its ground state, the identification of two positive-parity bands, of several low-lying levels, as well as the half-life of the band-head of the prolate band originated from the $\pi h_{11/2}$ configuration.

The ^{119}Cs nucleus was studied in an experiment using the ^{58}Ni(^{64}Zn, $3p$) fusion-evaporation reaction with a beam energy of 255 MeV and the JUROGAM 3+MARA setup at the Accelerator Laboratory of the University of Jyväskylä, Finland. A self-supporting enriched ^{58}Ni foil of 0.75 mg/cm^2 thickness was used as a target. The γ rays of ^{119}Cs have been identified by using the mass information provided by the in-flight double-focusing recoil mass separator MARA [19] and by the prompt X rays detected by the JUROGAM 3 array which was used to detect prompt γ rays [20]. No absorbers were mounted in front of the Ge detectors, which allowed the detection of γ rays with energies down to about 25 keV. Five clover germanium detectors surrounding the MARA focal-plane detection system were used to detect γ rays emitted by long-lived isomers and daughters of the β decay of the implanted recoils. A total of 4×10^{10} prompt γ-ray coincidence events with fold ≥ 3, not recoil gated, were collected. We first analyzed the recoil gated $\gamma\gamma\gamma$ coincidences. In a second step we analyzed the higher statistics prompt $\gamma\gamma\gamma$ coincidences without recoil gating, which made possible the identification of the weak transitions. More details of the experimental setup and data analysis can be found in Ref. [21].

Spin and parity assignments to newly observed levels are based on the measured two-point angular correlation (anisotropy) ratios R_{ac} [22,23]. The information on the observed transitions is given in Table 1 of the supplemental material. The partial level scheme of ^{119}Cs and a zoom on the low-lying states are given in Figs. 1 and 2. Spectra of Bands 1 and 3 are given in Fig. 3. Additional spectra are given in Figs. 1-4 of the supplemental material.

Two long-lived $9/2^+$ and $3/2^+$ isomers were known in ^{119}Cs before the present study, with deformations of $\beta = 0.336$ and $\beta = 0.296$, respectively, determined from the measured spectroscopic quadrupole moments [24]. The assigned $9/2^+$, $T_{1/2} = 40.0(2)$ s ground state was not determined experimentally, but based on systematics [17]. Both long-lived $9/2^+$ and $3/2^+$ isomers have been observed in the present experiment. However, the $\gamma\gamma\gamma$ coincidence relationships show clear evidence that the ground state of ^{119}Cs is instead the $3/2^+$, $T_{1/2} = 30.4(1)$ s state. It is fixed by the 209-keV $M1/E2$ transition depopulating the $5/2^+$ state of Band 5, and by the four parallel cascades 105-103, 41-103, 96-112 and (32)-112 keV depopulating the $5/2^+$ states of Bands 4 and 5. The spin-parities $(3/2^+)$ and $(1/2^+)$ of the 103- and 112-keV states, respectively, are tentatively assigned based on the angular correlations and the intensity balance of the feeding and depopulating transitions of the two states. The excitation energy of the $9/2^+$ isomer is established at 85.7 keV by the connecting transitions between Bands 8 and 6, which in turn decays to Band 4 through a 738.1-keV transition. The Bands 8 and 6 will be published separately in a forthcoming paper [21], in which the complete level scheme of ^{119}Cs will be reported.

The 110-keV energy of the $11/2^-$ band-head of Band 1 is fixed by five transitions between Bands 4 and 1. It decays to the $3/2^+$ ground state via the 87-keV transition detected at the MARA focal plane in delayed coincidence with γ rays of Band 1 measured at the target position (see Fig. 3 of supplemental material), and an unobserved (23)-keV transition. Another unobserved (25)-keV $E1$ transition can also exist between the 110-keV, $11/2^-$ state and the long-lived 86-keV $9/2^+$ band-head of Band 8 not shown in the present letter [25]. There are no other low-lying states to which the $11/2^-$ state can decay. As the systematics of low-lying states in odd-even Cs nuclei does not show very low-lying $7/2^+$ states [26], the (23)-keV transition is placed on top of the 87-keV transition. With such a placement, the low-energy (23)- and (25)-keV transitions can induce the observed isomeric character of the $11/2^-$ band-head of Band 1. A half-life of $T_{1/2} = 55(5)$ µs was deduced by fitting the time spectrum of the 87-keV γ ray (see Fig. 5 of the supplemental material). The 55 µs half-life is obviously for the 110-keV state, as the 87-keV $E2$ transition is too fast to generate such a long-living isomer. We tentatively assign spin and parity $(7/2^+)$ to the 87-keV state which leads to $M2$ character for the (23)-keV transition and $E1$ character for the (25)-keV transition. The Weisskopf estimates of these M2 and E1 transitions lead to a lifetime of the order of several tens of microseconds, which is in agreement with the measured half-life (more details are given in Ref. [21]).

The new Band 3 has been assigned to ^{119}Cs based on the mass 119 measured at the MARA focal plane in coincidence with band transitions and Cs X rays measured with JUROGAM 3. The 670-keV energy of the $11/2^-$ band-head is fixed by the cascade of transitions de-exciting the band towards the $3/2^+$ ground state. No transitions towards other low-lying states were observed. The intensity of the 268-, 237-, and 139-keV transitions depopulating the $11/2^-$ band-head is a factor of 16 lower than the intensity of the populating transitions, indicating an isomeric character with a lifetime in the range of tens of nanoseconds. The measured low intensity of the transitions depopulating the $11/2^-$ band-head is due to the emission by in-flight residual nuclei recoiling with a speed $v = 0.044$ c $= 1.3$ cm/ns, mainly out of the focus of JUROGAM 3, and therefore do not directly hitting the collimated and escape-suppressed HPGe detectors. The assigned negative parity to Band 3 is not firmly established, because the 294-keV transition is very weak and the (26)-keV transition to the 643-keV $9/2^+$ state is not observed. It is instead supported by the strongly-coupled

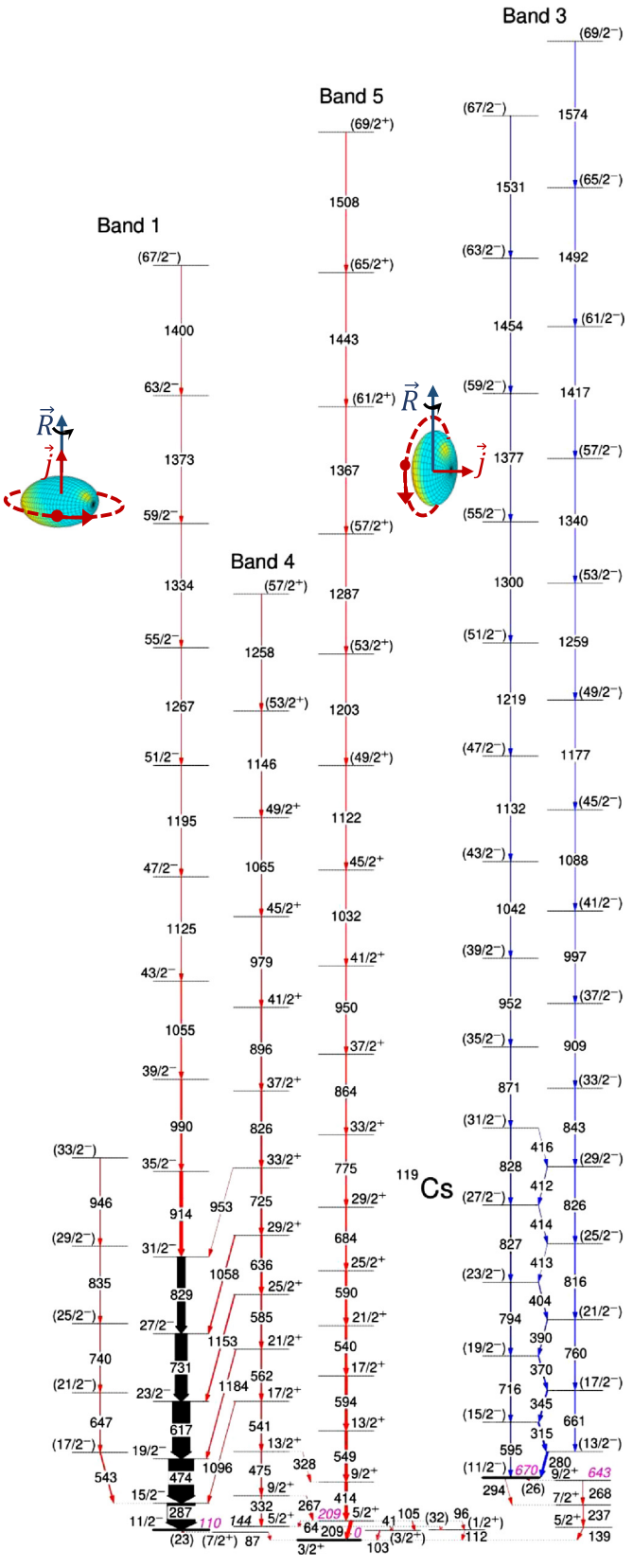

Fig. 1. Partial level scheme of ^{119}Cs showing the Bands 1, 3, 4 and 5. The prolate shapes assigned to Bands 1, 4, 5 and the oblate shape assigned to Band 3, as well as the orbits and angular momenta of the odd proton are schematically drawn. The new transitions are indicated in red or blue. The isomeric levels are indicated with thick lines. The bands continue at higher spins with the transitions listed in Table 1 of the supplemental material.

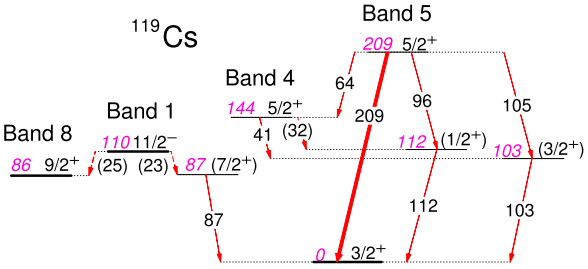

Fig. 2. Zoom on the low-lying part of the level scheme.

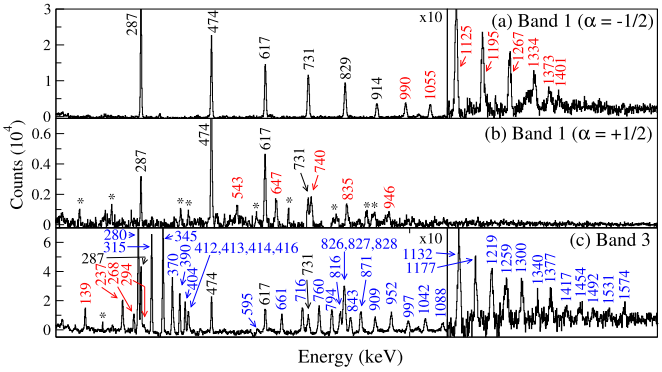

Fig. 3. Double-gated spectra for Bands 1 and 3 of ^{119}Cs. Peak energies are written in black for previously known transitions, and in red or blue for the newly identified ones. Transitions from other nuclei (^{116}Xe, ^{118}Xe, ^{119}Ba, ^{120}Ba) are indicated with an asterisk, while those from other bands in ^{119}Cs (Bands 2 and 8) are indicated with a circle. The lists of gating transitions for each spectrum are given in the supplemental file.

character of the band which implies the occupation of a high-Ω orbital. As for prolate deformation the only high-Ω orbital close to the $Z = 55$ Fermi surface is $[404]9/2^+$ which is assigned to Band 8 [27,21], the configuration of Band 3 can only be based on the $\pi h_{11/2}[505]11/2^-$ orbital which is close to the Fermi surface for oblate deformation, giving thus confidence in the assigned negative parity. The decay of Band 3 only towards the three $5/2^+$, $7/2^+$ and $9/2^+$ states below the band-head, and the lack of connecting transitions between these states and the other positive-parity states, strongly suggests that these states are also based on oblate shapes, associated to the occupation of the $\pi[413]5/2^+$ and/or $\pi[402]5/2^+$ orbitals close to the Fermi surface for oblate deformation (see the following and Fig. 9(c) of the supplemental material.)

The new Bands 4 and 5 are also assigned to ^{119}Cs based on the mass 119 measured at the MARA focal plane in coincidence with band transitions and Cs X rays measured with JUROGAM 3, and subsequently confirmed by the connecting transitions with Band 1 (see Fig. 3 and Fig. 2 of the supplemental material), which are not strong enough to allow the extraction of the polarization asymmetry and therefore their electromagnetic character. However, as in the case of the other bands, the weakest transitions have been identified by analyzing the $\gamma\gamma\gamma$ coincidences without recoil gating. The assigned positive parity to Band 4 is based on the properties of the band, which, being composed of only one cascade of $E2$ transitions, indicates the occupation of a low-Ω orbital with signature $\alpha = 1/2$, most probably $\pi[420]1/2^+$. The particle number conserving cranked shell-model (PNC-CSM) calculations [28,29] for the $\pi[420]1/2^+(\alpha = 1/2)$ configuration are in excellent agreement with Band 4, showing the alignment of a proton pair at ≈ 0.35 MeV/$\hbar$, followed by a more gradual alignment of a pair of neutrons at $\hbar\omega \approx 0.50$ MeV/$\hbar$ (see Fig. 6 of the supplemental material). The spins and positive parity of Band 5 are fixed by the connecting $E2$ transitions with Band 4. Based on the good agreement between

the PNC-CSM calculations and the experimental band, we assign the $\pi[422]3/2^+(\alpha = 1/2)$ configuration to Band 5.

Band 1 previously known up to spin $35/2^-$ [27], is now extended up to spin $(67/2^-)$. We also identified a weakly populated band decaying to the $15/2^-$ state of Band 1, which we assigned as the unfavored signature partner of Band 1.

The proton-rich $A \approx 120$ nuclei are well deformed. The deformation parameters employed in the band-head calculations were in the past smaller by 10% to 20% than the deformation parameters deduced from isotope shifts and spectroscopic quadrupole moments [27]. This has an important effect on the assigned configurations, in particular for the bands built on the $h_{11/2}$ orbital in Cs nuclei: for a deformation $\beta_2 \approx 0.25$ resulting from TRS calculations [27], the $\pi[550]1/2^-$ orbital is closest to the Fermi surface, while if one uses the deformation $\beta_2 \approx 0.336$ deduced from experiment [24], the $\pi[541]3/2^-$ orbital is closest to the Fermi surface.

The negative-parity Band 3 is assumed to have oblate shape. It does not decay to the other negative-parity bands, which are all consistently interpreted as built on prolate shape. This can be explained by the existence of a barrier between the oblate and prolate minima, which can be as high as 5 MeV [14,12,13], but also by a very different orientation of the spin of the odd proton relative to the core which can lead to ΔK forbidden transitions. It also does not decay to the low-lying states populated by transitions from Bands 4 and 5, which are also based on prolate shapes. One can therefore speculate that the decay of Band 3 proceeds towards states built on the same oblate shape, with configurations built on $\pi[413]5/2^+$ and $\pi[402]5/2^+$ orbitals close to the Fermi surface for an oblate deformation of $\varepsilon_2 \approx -0.2$. The missing high-$\Omega$ orbitals close to the $Z = 55$ Fermi surface for a prolate deformation of $\varepsilon_2 \approx 0.3$, which can explain the observed decay of Band 3, are another argument in favor of oblate shapes assigned to Band 3 and to the positive-parity states towards which it decays.

The potential energy surface of ^{119}Cs for the $\pi h_{11/2}$ configuration calculated by the tilted axis cranking covariant density functional theory (TAC-CDFT) [30–32] is shown in Fig. 4. The density functional PC-PK1 [33] is used in the particle-hole channel, and it has been successfully used to describe not only the ground-state properties including the nuclear masses [34–36] and quadrupole moments [37], but also nuclear rotations such as magnetic and antimagnetic rotations [30,38–40], chiral rotations [41], etc. For the particle-particle channel, a finite-range separable pairing force [42] is employed. As one can see from Fig. 4, the potential energy surface exhibits a minimum around $\beta \approx 0.3$ and is very soft in the γ direction. The energy minimum pathway demonstrates that the oblate shape is favored for β smaller than 0.2 corresponding to the observed Band 3, and the prolate shape becomes favored for larger β values, corresponding to Band 1. These features support the coexistence of prolate and oblate minima, however without a separating barrier between them. Note that beyond-mean-field correlations induced by the rotational symmetry restoration and the shape fluctuation, which are missing in the present calculations, would play a role in the shape coexistence. Further investigations by the five dimensional collective Hamiltonian approach [43,44] could be very interesting.

As one can see in Fig. 5, the theoretical moments of inertia $J^{(1)}$ and projection of the total spin on the cranking axis J_x calculated assuming $\varepsilon_2 = 0.32$ for Band 1 (taken from the measured quadrupole moment of the $9/2^+$ isomer [24]), and $\varepsilon_2 = -0.17$ for Band 3 (taken from the TAC-CDFT results), are in good agreement with the experimental values. They show a sharp proton alignment accompanied by a gradual neutron alignment in the favored signature partner of Band 1. The same good agreement is achieved for Bands 4 and 5 calculated for a deformation of $\varepsilon_2 \approx 0.32$ (see Figs. 6 and 7 of the supplemental material), which reveal a sharp proton alignment at $\hbar\omega \approx 0.3$ MeV followed by a more gradual

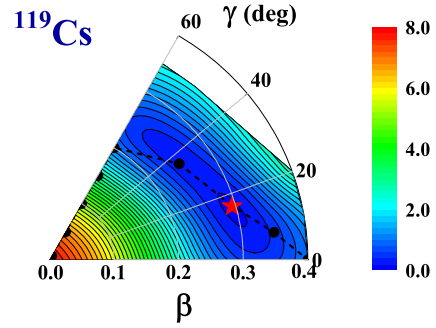

Fig. 4. The potential energy surface of ^{119}Cs in the β-γ deformation plane for the configuration $\pi h_{11/2}$ calculated by the TAC-CDFT. The energy separation between contour lines is 0.2 MeV. The energy minimum pathway and the position of absolute energy minimum are denoted by black dots and red star, respectively.

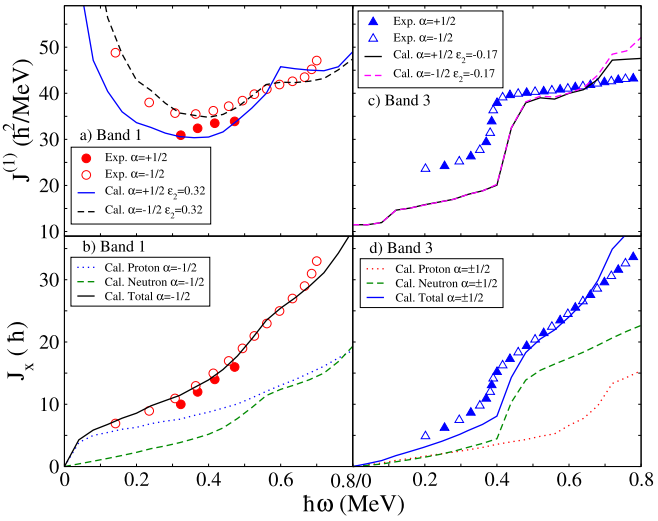

Fig. 5. a) and c) Moments of inertia $J^{(1)}$, b) and d) projections of the angular momentum on the cranking axis J_x for Bands 1 and 3 of ^{119}Cs calculated using the PNC-CSM model assuming axially symmetric shapes. The states with signature $\alpha = +1/2$ and $\alpha = -1/2$ are drawn with filled and open symbols, respectively.

neutron alignment at $\hbar\omega \approx 0.5$ MeV. A smaller deformation for the positive-parity Bands 4 and 5 can be excluded, since in that case the neutron alignment is calculated sharper than experimentally observed (see in Fig. 7 of the supplemental material).

In summary, the present work reports for the first time evidence of oblate-prolate shape coexistence close to the ground state in the strongly-deformed ^{119}Cs nucleus. Theoretical calculations performed with TAC-CDFT and PNC-CSM reproduce the salient features of the experimental data. The present results open the way to further experimental and theoretical investigations of $A \approx 120$ nuclei close to the proton drip line, for which ground-state oblate shapes are predicted.

Declaration of competing interest

The authors declare that they have no known competing financial interests or personal relationships that could have appeared to influence the work reported in this paper.

Acknowledgements

This work has been supported by the China Scholarship Council (CSC), CSC No. 201804910386. This work has been supported by the Academy of Finland under the Finnish Centre of Excellence Programme (2012-2017), by the EU 7th Framework Programme Project No. 262010 (ENSAR), by the United Kingdom Science and

Technology Facilities Council; by the National Research, Development and Innovation Fund of Hungary (Project No. K128947), as well as by the European Regional Development Fund (Contract No. GINOP-2.3.3-15-2016-00034); by the Swedish Research Council under Grant No. 2019-04880; and by the National Natural Science Foundation of China (Grants No. 11505242, No. 11305220, No. U1732139, No. 11775274, and No. 11575255). C.A. is supported by the Natural Sciences and Engineering Research Council of Canada. The use of germanium detectors from the GAMMAPOOL is acknowledged. I.K. was supported by National Research, Development and Innovation Office-NKFIH, contract number PD 124717.

Appendix A. Supplementary material

Supplementary material related to this article can be found online at https://doi.org/10.1016/j.physletb.2021.136645.

References

[1] A.N. Andreyev, et al., Nature 404 (2000) 430, https://doi.org/10.1038/35013012.
[2] J. Pakarinen, et al., Phys. Rev. C 72 (2005) 011304(R), https://doi.org/10.1103/PhysRevC.72.011304.
[3] H. Hubel, et al., Nucl. Phys. A 453 (1986) 316, https://doi.org/10.1016/0375-9474(86)90014-X.
[4] D. Ye, et al., Phys. Lett. B 236 (1990) 7, https://doi.org/10.1016/0370-2693(90)90585-T.
[5] S.M. Fischer, et al., Phys. Rev. Lett. 84 (2000) 4064, https://doi.org/10.1103/PhysRevLett.84.4064.
[6] E. Clement, et al., Phys. Rev. C 75 (2007) 054313, https://doi.org/10.1103/PhysRevC.75.054313.
[7] K. Heyde, J.L. Wood, Rev. Mod. Phys. 83 (2011) 1467, https://doi.org/10.1103/RevModPhys.83.1467.
[8] E.S. Paul, et al., Phys. Rev. Lett. 58 (1987) 984, https://doi.org/10.1103/PhysRevLett.58.984.
[9] U.S. Tandel, et al., Phys. Rev. Lett. 101 (2008) 182503, https://doi.org/10.1103/PhysRevLett.101.182503.
[10] C.M. Petrache, et al., Phys. Rev. C 99 (2019) 041301(R), https://doi.org/10.1103/PhysRevC.99.041301.
[11] P. Möller, et al., At. Data Nucl. Data Tables 94 (2008) 758, https://doi.org/10.1016/j.adt.2008.05.002.
[12] L.M. Robledo, et al., Phys. Rev. C 78 (2008) 034314, https://doi.org/10.1103/PhysRevC.78.034314.
[13] H.L. Wang, et al., Phys. Rev. C 92 (2015) 024303, https://doi.org/10.1103/PhysRevC.92.024303.
[14] http://www-phynu.cea.fr/science_en_ligne/carte_potentiels_microscopiques/carte_potentiel_nucleaire_eng.htm.
[15] G.A. Lalazissis, D. Vretenar, P. Ring, Nucl. Phys. A 650 (1999) 133, https://doi.org/10.1016/S0375-9474(99)00121-9.
[16] M. Aggarwal, Phys. Rev. C 89 (2014) 024325, https://doi.org/10.1103/PhysRevC.89.024325.
[17] D.M. Symochko, E. Browne, J.K. Tuli, Nucl. Data Sheets 110 (2009) 2945–3105, https://doi.org/10.1016/j.nds.2009.10.003.
[18] N.J. Stone, At. Data Nucl. Data Tables 90 (2005) 75–176.
[19] J. Sarén, et al., Nucl. Instrum. Methods Phys. Res., Sect. A 266 (2008) 4196, https://doi.org/10.1016/j.nimb.2008.05.027.
[20] J. Pakarinen, et al., Eur. Phys. J. A 56 (2020) 149, https://doi.org/10.1140/epja/s10050-020-00144-6.
[21] K.K. Zheng, et al., to be published.
[22] V. Iacob, G. Duchene, Nucl. Instrum. Methods Phys. Res., Sect. A 399 (1) (1997) 57–64, https://doi.org/10.1016/S0168-9002(97)00872-3, http://www.sciencedirect.com/science/article/pii/S0168900297008723.
[23] K. Starosta, et al., Nucl. Instrum. Methods Phys. Res., Sect. A 423 (1) (1999) 16–26, https://doi.org/10.1016/S0168-9002(98)01220-0.
[24] C. Thibault, et al., Nucl. Phys. A 367 (1981) 1–12, https://doi.org/10.1016/0375-9474(81)90274-8.
[25] K.K. Zheng, et al., to be published.
[26] A. Gizon, et al., Eur. Phys. J. A 8 (2000) 41, https://doi.org/10.1007/s10050-000-4503-0.
[27] F. Lidén, et al., Nucl. Phys. A 550 (1992) 365–390, https://doi.org/10.1016/0375-9474(92)90687-F.
[28] J.Y. Zeng, T.H. Jin, Z.J. Zhao, Phys. Rev. C 50 (1994) 1388, https://doi.org/10.1103/PhysRevC.50.1388.
[29] Z.H. Zhang, M. Huang, A.V. Afanasjev, Phys. Rev. C 101 (2020) 054303, https://doi.org/10.1103/PhysRevC.101.054303.
[30] P.W. Zhao, S.Q. Zhang, J. Peng, H.Z. Liang, P. Ring, J. Meng, Novel structure for magnetic rotation bands in ^{60}Ni, Phys. Lett. B 699 (3) (2011) 181–186, https://doi.org/10.1016/j.physletb.2011.03.068.
[31] J. Meng, J. Peng, S.Q. Zhang, P.W. Zhao, Progress on tilted axis cranking covariant density functional theory for nuclear magnetic and antimagnetic rotation, Front. Phys. 8 (2013) 55–79, https://doi.org/10.1007/s11467-013-0287-y.
[32] Y.K. Wang, Yrast band of ^{109}Ag described by tilted axis cranking covariant density functional theory with a separable pairing force, Phys. Rev. C 96 (2017) 054324, https://doi.org/10.1103/PhysRevC.96.054324, https://link.aps.org/doi/10.1103/PhysRevC.96.054324.
[33] P.W. Zhao, Z.P. Li, J.M. Yao, J. Meng, New parametrization for the nuclear covariant energy density functional with a point-coupling interaction, Phys. Rev. C 82 (2010) 054319, https://doi.org/10.1103/PhysRevC.82.054319.
[34] K.Q. Lu, Z.X. Li, Z.P. Li, J.M. Yao, J. Meng, Global study of beyond-mean-field correlation energies in covariant energy density functional theory using a collective Hamiltonian method, Phys. Rev. C 91 (2015) 027304, https://doi.org/10.1103/PhysRevC.91.027304, https://link.aps.org/doi/10.1103/PhysRevC.91.027304.
[35] P.W. Zhao, L.S. Song, B. Sun, H. Geissel, J. Meng, Crucial test for covariant density functional theory with new and accurate mass measurements from Sn to Pa, Phys. Rev. C 86 (2012) 064324, https://doi.org/10.1103/PhysRevC.86.064324, https://link.aps.org/doi/10.1103/PhysRevC.86.064324.
[36] Y.L. Yang, Y.K. Wang, Nuclear chart in covariant density functional theory with dynamic correlations: from oxygen to tin, Chin. Phys. C 44 (3) (2020) 034102, https://doi.org/10.1088/1674-1137/44/3/034102.
[37] P.W. Zhao, S.Q. Zhang, J. Meng, Explanation of the simplicity of the quadrupole moments recently observed in Cd isotopes from covariant density functional theory, Phys. Rev. C 89 (2014) 011301, https://doi.org/10.1103/PhysRevC.89.011301, https://link.aps.org/doi/10.1103/PhysRevC.89.011301.
[38] P.W. Zhao, J. Peng, H.Z. Liang, P. Ring, J. Meng, Antimagnetic rotation band in nuclei: a microscopic description, Phys. Rev. Lett. 107 (2011) 122501, https://doi.org/10.1103/PhysRevLett.107.122501.
[39] P.W. Zhao, J. Peng, H.Z. Liang, P. Ring, J. Meng, Covariant density functional theory for antimagnetic rotation, Phys. Rev. C 85 (2012) 054310, https://doi.org/10.1103/PhysRevC.85.054310.
[40] Y.K. Wang, Magnetic rotations in ^{198}Pb and ^{199}Pb within covariant density functional theory with pairing correlations, Phys. Rev. C 97 (2018) 064321, https://doi.org/10.1103/PhysRevC.97.064321, https://link.aps.org/doi/10.1103/PhysRevC.97.064321.
[41] P.W. Zhao, Multiple chirality in nuclear rotation: a microscopic view, Phys. Lett. B 773 (Supplement C) (2017) 1–5, https://doi.org/10.1016/j.physletb.2017.08.001.
[42] Y. Tian, Z. Ma, P. Ring, A finite range pairing force for density functional theory in superfluid nuclei, Phys. Lett. B 676 (1–3) (2009) 44–50, https://doi.org/10.1016/j.physletb.2009.04.067.
[43] T. Nikšić, Z.P. Li, D. Vretenar, L. Próchniak, J. Meng, P. Ring, Beyond the relativistic mean-field approximation. iii. Collective Hamiltonian in five dimensions, Phys. Rev. C 79 (2009) 034303, https://doi.org/10.1103/PhysRevC.79.034303, https://link.aps.org/doi/10.1103/PhysRevC.79.034303.
[44] Z.P. Li, T. Nikšić, D. Vretenar, J. Meng, G.A. Lalazissis, P. Ring, Phys. Rev. C 79 (2009) 054301, https://doi.org/10.1103/PhysRevC.79.054301.